

Manuscript Number:

Title: Adaptive self-configuring computer vision system for quality evaluation of fresh-cut radicchio

Article Type: Research Article

Keywords: Computer vision system, non-destructive quality evaluation, self-configuration, automatic colors and features selection, image analysis.

Corresponding Author: Dr. Maria Cefola, Ph.D

Corresponding Author's Institution: ISPA

First Author: Bernardo Pace

Order of Authors: Bernardo Pace ; Dario P Cavallo; Maria Cefola, Ph.D; Roberto Colella; Giovanni Attolico

Abstract: An innovative Computer Vision System (CVS) that extracts color features discriminating the quality levels occurring during fresh-cut radicchio storage in air or modified atmosphere packaging was proposed. It self-configures the parameters normally set by operators and completely automates the following steps adapting to the specific product at hand: color-chart detection, foreground extraction and color segmentation for features extraction and selection. Results proved the average value of a^* over the white part and the percentage of light white with respect to the whole visible surface to be the most discriminating color features to significantly separate ($P \leq 0.05$) the three desired quality levels (high, middle and poor) occurring during fresh-cut radicchio storage (whose true value was verified on the base of ammonium content and human evaluated visual quality). The proposed procedure significantly simplify the CVS design and the optimization of its performance, limiting the subjective human intervention to the minimum.

D. Knorr

Editor

Innovative Food Science and Emerging Technologies

Bari, 09/07/2015

Dear Prof. Knorr,

I am pleased to submit the paper entitled “**Adaptive self-configuring computer vision system for quality evaluation of fresh-cut radicchio**” by Pace Bernardo, Cavallo Dario Pietro , Cefola Maria, Colella Roberto & **Attolico Giovanni** for publication in the journal **Innovative Food Science and Emerging Technologies**.

Please find my complete address below:

Maria Cefola Ph.D.

Consiglio Nazionale delle Ricerche C.N.R.

Istituto di Scienze delle Produzioni Alimentari

Via G. Amendola 122/O, 70126 Bari - ITALY

Phone +39 080.592.9304

e-mail maria.cefola@ispa.cnr.it

Sincerely,

Maria Cefola

Industrial relevance

The non-destructive quality control represents a valuable tool to monitor fruits and vegetables along the whole chain from production to the end-user. Increased consumers' satisfaction and reduction of waste are just two examples of benefits that can come from a frequent and consistent control of food. CVS represent the most powerful and flexible way to reach these results. The current state-of-the-art make their design strongly related to the specific product at hand. Thresholds and features are characteristics that play a critical role in determining the final performance of system but are generally set by designers or operators using a-priori knowledge and/or trial-and-error processes. The proposed innovative procedure allows the CVS to self-configure most of these parameters and to easily adapt to different products regardless of the number and kind of colors associated to their surface. It results of practical applications in food processing, providing a non-destructive, automatic, cheap, fast and simple technology for the quality level evaluation, whose configuration requires a reduced, less critical and less technical human intervention.

Highlights

1. Computer Vision System for the no-destructive and automatic color analysis
2. Automatic color-chart location and separation of foreground from background
3. Automatic identification of color features able to evaluate product quality
4. Light White percentage discriminated fresh-cut radicchio quality levels
5. CVS was able to identify quality of fresh-cut radicchio stored in AIR or pMA

Adaptive self-configuring computer vision system for quality evaluation of fresh-cut radicchio

Pace Bernardo ^{a1}, Cavallo Dario Pietro ^{b1}, Cefola Maria ^{a1*}, Colella Roberto ^b,

Attolico Giovanni ^b

^a Institute of Sciences of Food Production, CNR-National Research Council of Italy Via G. Amendola, 122/O – 70126 Bari, Italy

^b Institute on Intelligent Systems for Automation, CNR-National Research Council of Italy Via G. Amendola, 122/O – 70126 Bari, Italy

* Corresponding Author: phone/fax: +39.080.5929304/9374; e-mail address: maria.cefola@ispa.cnr.it

¹ First Authorship is equally shared

Abstract

An innovative Computer Vision System (CVS) that extracts color features discriminating the quality levels occurring during fresh-cut radicchio storage in air or modified atmosphere packaging was proposed. It self-configures the parameters normally set by operators and completely automates the following steps adapting to the specific product at hand: color-chart detection, foreground extraction and color segmentation for features extraction and selection. Results proved the average value of a^* over the white part and the percentage of light white with respect to the whole visible surface to be the most discriminating color features to significantly separate ($P \leq 0.05$) the three desired quality levels

23 (high, middle and poor) occurring during fresh-cut radicchio storage (whose true value was verified
24 on the base of ammonium content and human evaluated visual quality). The proposed procedure
25 significantly simplify the CVS design and the optimization of its performance, limiting the subjective
26 human intervention to the minimum.

27 **Industrial relevance**

28 The non-destructive quality control represents a valuable tool to monitor fruits and vegetables along
29 the whole chain from production to the end-user. Increased consumers' satisfaction and reduction of
30 waste are just two examples of benefits that can come from a frequent and consistent control of food.
31 CVS represent the most powerful and flexible way to reach these results. The current state-of-the-art
32 make their design strongly related to the specific product at hand. Thresholds and features are
33 characteristics that play a critical role in determining the final performance of system but are generally
34 set by designers or operators using a-priori knowledge and/or trial-and-error processes. The proposed
35 innovative procedure allows the CVS to self-configure most of these parameters and to easily adapt to
36 different products regardless of the number and kind of colors associated to their surface. It results of
37 practical applications in food processing, providing a non-destructive, automatic, cheap, fast and
38 simple technology for the quality level evaluation, whose configuration requires a reduced, less
39 critical and less technical human intervention.

40

41 **Keywords:** Computer vision system, non-destructive quality evaluation, self-configuration, automatic
42 colors and features selection, image analysis.

43

44 **1. Introduction**

45 In the last years, due to the increased consumers' requests for quality, the food industry has paid great
46 attention to measure and control the visual appearance of products (Wu & Sun, 2013a; Zhang et al.,
47 2014). As regards fruits and vegetables, visual appearance is normally strongly related to overall

48 quality and is therefore a very useful method to judge the quality level. In particular, in these products,
49 accurate measurements of some chromatic properties (such as intensity, hue, chroma, color
50 uniformity) provide important indicators of visual appearance. Generally, bright and vivid colors are
51 associated with freshness and better quality, while dull colors are a normal consequence of an overall
52 quality loss (Nunes, 2015). It has been proved that specific color features are correlated with quality
53 level of fruits and vegetables. Pace et al. (2011, 2014a) reported a strong relationship of visual
54 appearance with and b^* (or Chroma) in fresh-cut nectarines and with brown pigments in lettuce.
55 Similarly, Nunes (2015) found significant correlations between color parameters and visual
56 appearance in many fruits and vegetables. Generally, the color parameters related to visual appearance
57 are manually acquiring by colorimeter in a proper set of sample points on the product's surface.
58 Recently, there is an increasing attention to the use of computer vision systems (CVS). CVS are more
59 vulnerable to instabilities of the acquisition environment than colorimeters but, if properly calibrated
60 and used, proved to be more robust, since they can analyze the complete surface of the product and
61 are not affected by the arbitrary and subjective choice of sampling points (Pace et al., 2011, 2013,
62 2014a; Wu & Sun 2013a; Zhang et al., 2014; Manninen et al., 2015). CVS can extract from an image
63 several features including color histograms, presence and size of defective areas and color texture
64 (Hernández-Carrión et al., 2015). However, it is important to highlight that, in several cases, only
65 specific color features, are well related to the quality (Pace et al., 2014a).

66 Starting from these considerations, the automatic identification of the most discriminative colors by
67 CVS could improve the non-destructive quality level evaluation of fruits and vegetables, reducing the
68 error due to subjective identification of the most discriminating colors (and of related parameters) of
69 the overall quality level. Automatic quality classification, based on image analysis was reported by
70 Zhang et al., (2014). In addition, Kordecki & Palus (2014) reported an automatic color-chart detection
71 algorithm that determines the type and locations of color-patches in images. Color-charts are placed in
72 the scene to provide reference colors that enable the evaluation and the reduction of effects of

73 acquisitions environment on the behavior of the CVS. The algorithm, proposed by Kordecki & Palus
74 (2014), used k-means clustering to accomplish color quantization and segmentation of a collection of
75 regions some of which are the color-chart's patches. Further criteria, inspired by the a-priori
76 knowledge about the structure of the color-chart (shape, number, position, shape and size of patches)
77 were used to select and to identify the color-chart. Recently, Zhang et al. (2015) proposed a CVS to
78 automatically detect defective apples by combining background removal, automatic correction of
79 lightness, counting defected regions and a relevance vector machine (RVM) classifier. The system
80 used a camera that acquires RGB and NIR (Near InfraRed) registered images of the same scene. The
81 binary mask of the foreground was obtained using a (experimentally identified) threshold on the NIR
82 image. A morphological filling was therefore applied to increase the quality of the segmented region.
83 A lightness correction was applied in the peripheral part of the apple to compensate for the change of
84 geometry between light, camera and surface. Moreover, Avila et al. (2015) proposed an automatic
85 method to construct olives' and grape seeds' color scales maturity: the system used an illumination
86 invariant color model and the threshold for foreground segmentation was determined using the Otsu's
87 method (Otsu, 1975). However, most of the cited literature is related to products characterized by
88 mostly homogeneous color. The evaluation of color change in products characterized by nonuniform
89 color is still a critical task (Balaban, 2008; Wu & Sun; 2013a).

90 Starting from these findings, in this paper an automatic procedure for the non-destructive extraction
91 by CVS of color features was proposed and applied for the evaluation of the quality level during
92 storage of the fresh-cut radicchio, characterized by nonuniform color.

93

94 **2. Materials and Methods**

95 *2.1. Plant material and processing*

96

97 Radicchio di Chioggia heads (*Cichorium intybus* L. group *rubifolium*) belonging to two hybrids
98 (Corelli and Botticelli), were provided in two different harvest times by a farm located in
99 Pontecagnano (south Italy) and immediately transported in cold condition to the Postharvest

100 Laboratory of the Institute of Sciences of Food Production. Heads of each hybrid were selected to
101 discard damaged samples and processed as fresh-cut product. In detail, radicchio heads were prepared
102 by removing and discarding wrapper leaves and the stem with sharp stainless steel knives. Radicchio
103 pieces (3 × 4 cm), obtained by using a vegetable cutter (CL52 Robot Coupe, Vincennes-Cedex,
104 France), were pooled and blended to minimize product heterogeneity. Radicchio pieces were washed
105 in tap water at 4 °C for 4 min. After washing, pieces were dried using a manual centrifuge and
106 packaged in polypropylene bags (25 × 30 cm, 30 µm, Carton Pack, Rutigliano, Italy) containing each
107 one about 150 g of product either sealed in passive modified atmosphere (pMA, at equilibrium: 10%
108 O₂ and 7% CO₂) or in unsealed bags (AIR). In total, 120 bags (two radicchio hybrids x six replicates ×
109 five quality levels x two packaging condition) were prepared and stored at 4 (± 1.0) °C. All items, at
110 proper times during storage, were graded using a five quality level scale, based on sensory evaluation,
111 as reported below. Images of samples belonging to each quality level were acquired and processed by
112 Computer vision system (CVS); moreover the same samples underwent a chemical analysis for the
113 ammonium content (NH₄⁺).

114

115 2.2. *Quality level classification and NH₄⁺ analysis*

116

117 Along the storage, fresh-cut radicchio were classified using five quality levels (QL) according to the
118 following scale: 5 = very good (very fresh, no signs of wilting, decay or bruises), 4 = good (slight
119 signs of shrivelling, bruises), 3 = limit of acceptability or marketability (moderate signs of shrivelling,
120 browning, dryness, wilting, bruises), 2 = poor (severe bruises, evident signs of shrivelling, pitting,
121 decay), and 1 = very poor (unacceptable quality due to decay, bruises, leaky juice). The QL 3 was
122 considered the minimum threshold of acceptance for sale or consumption (Nunes et al., 2009).

123 For NH₄⁺ analysis the method reported by Pace et al. (2014a) was used. In detail, five g of chopped
124 sample was extracted in distilled water and, after the reaction with nitroprusside reagent and alkaline

125 hypochlorite solution, color development was determined after incubation at 37 °C for 20 min,
126 reading the absorbance at 635 nm (UV-1800, Shimadzu, Kyoto, Japan).

127

128 2.3. *Color analysis by computer vision system (CVS)*

129

130 2.3.1. *CVS description and setup*

131

132 The images used in the experiments were acquired using a 3CCD (Charged Coupled Device) digital
133 camera (JAI CV-M9GE). The camera has a dedicated CCD for each color channel and provides a
134 reliable color measure at full resolution, without the artifacts of most digital cameras (based on the
135 Bayer filter). The uncompressed TIFF format was used to save images while avoiding any color
136 artifacts produced by lossy compression algorithms. The camera mounted a Linos MeVis 12 mm lens
137 system whose optical axis was perpendicular to the black background onto which the products were
138 placed. Eight halogen lamps, divided along two rows placed at the two sides of the imaged area, were
139 used. They were oriented using a 45° angle with respect to the optical axis of the CCD camera and to
140 the plane on which the products were placed (Pace et al., 2014a).

141 2.3.2. *Color-chart detection*

142

143 A small color-chart (X-Rite Color Control Patches, Fig. 1) has been placed in the scene during the
144 acquisition of each image. Its patches allow the estimation and reduction of color variations occurring
145 in time due to the behavior of CVS components and to uncontrollable changes of environmental
146 conditions. X-Rite releases the numerical values associated to the color of each patch in the CIE
147 $L^*a^*b^*$ space. To use this information, the detection of the color-chart and the identification of each
148 patch are needed when processing each image: to make these two steps automatic strongly simplify
149 the processing of images, without requiring human intervention. The implemented method looked for
150 two achromatic patches (the white 19th and the light grey 20th) using an iterative process that
151 considered color, shape and size. When satisfactorily results were found, their central positions were

152 used to look for the position of the 13th patch, placed at 90 degrees with respect to the vector
153 connecting the white and the light grey patches. Then all the other patches were identified in a
154 straightforward way using the knowledge about the structure of the color chart. The measured $L^*a^*b^*$
155 values and the expected ones (supplied by X-Rite) were used to estimate and correct as much as
156 possible any difference induced by environmental conditions and sensor characteristics. The white
157 patch was also used to white-balance the image: a correction coefficient was evaluated for each band
158 to reduce the distance between the measured white and the reference one. Each coefficient was
159 therefore applied to the corresponding band over the whole image. In Fig. 2 some steps of this
160 procedure are showed. The source image and the automatically detected 19th and 20th patches are
161 shown in Fig. 2A and 2B respectively; Fig. 2C shows how all the patches are isolated to measure the
162 corresponding color. Finally, in Fig. 2D, the source image in which the detected color-chart has been
163 removed is reported. The detection and extraction of color-chart does not make any assumption about
164 its position and attitude inside the scene and can be fruitfully used in more general applications and
165 different contexts.

166 2.3.3. *Foreground extraction*

167
168 After the detection (and subsequent removal) of the color-chart, the separation of the product at hand
169 (foreground) from the image background was needed. In our previous work, such separation was
170 achieved using a threshold fixed experimentally (Pace et al., 2013). The new version of the CVS
171 automatized this step. For each pixels (p_{ij}) of the image, the Euclidean distances with respect to its
172 neighbors in an 8-neighborhood was evaluated using the saturation channel in the HSV (Hue
173 Saturation Brithness) color space; then the histogram of these distances over the whole image was
174 built. A typical result is shown in Fig. 3. Two Gaussian distributions were fitted to the histogram: the
175 first (denoted fit_1 and associated to homogeneous regions) with a peak around 0 is mainly related to
176 regions of the image such with small variations in color as the background. The second (denoted fit_2
177 and associated to edges) is due to strong color variations occurring at the edges that separate

178 foreground and background. Considering fit_1 and fit_2 to be two Gaussian distributions (with means μ_1
179 and μ_2 and variances σ_1 and σ_2 respectively, fit_2 was obtained excluding the data in the histogram
180 lower than $\mu_1 + 2*\sigma_1$. Finally, $\mu_2 - \sigma_2/2$ was used as the threshold selecting the strong edges between
181 foreground and background, where the correction $\sigma_2/2$ was introduced to account for the effects of
182 possible noise caused by pixels that were close to edges. This conservative choice was done since
183 losing some foreground pixels was less dangerous than including by mistake background pixels in
184 the foreground region (Fig. 4). Fig. 4 shows this process; in particular, in Fig. 4A-B the results
185 obtained by applying a quite high (fixed) threshold on the three color channels are showed: only the
186 pixels whose color components were all above the threshold were set to foreground. This very
187 conservative choice was independent from product and acquisition environment but separated only a
188 quite small part of the product's surface, assigning to the background all the pixels having even a
189 single color channel below the specified value. This preliminary result collected only pixels certainly
190 belonging to the product surface: it was used as seed for the following growing schema. These
191 original regions were extended by including all the neighboring pixels whose colors differed from the
192 pixels already classified as foreground by a value lower than a threshold. The value of this threshold
193 was fixed using a bottom-up, data-driven approach that automatically adapted to different products
194 and images. The result (Fig. 4 C-D) shows that some small areas of product were erroneously
195 classified as background. The proposed method did not apply any morphological processing to fill
196 these gaps and holes.

197 2.3.4. *Color segmentation*

198

199 Partitioning of an image into disjoint and homogeneous regions with respect to characteristics of
200 interest is often necessary to accomplish useful measurements with a CVS. In this work, the
201 identification and separation of the two relevant colors (white and red) of fresh-cut radicchio was
202 needed to measure their changes separately. A hierarchical clustering technique was used to segment
203 colors: this technique does not require any initialization and builds a structure that can be used to

204 dynamically select different resolutions of segmentation according to the requirements of the
205 application at hand.

206 During the processing of each image, the colors expressed in the RGB space of all the pixels
207 belonging to the foreground were converted into the CIE $L^*a^*b^*$ color space, chosen for its perceptual
208 uniformity and device independency (Kang et al., 2008). The channel L^* (representing lightness), as
209 known is less reliable. The other two channels were quantized (using mathematical rounding) to
210 reduce the number of possible a^* and b^* pairs. A two dimensional histogram such as the one shown in
211 Fig. 5 was produced, where the third dimension represents the percentage of occurrences of the
212 corresponding (a^*, b^*) pair in the foreground region. The histograms of all the available images were
213 therefore analysed to compute the variance of the number of occurrences at every single (a^*, b^*) pair
214 over the whole dataset. A predefined number of (a^*, b^*) pairs were therefore selected choosing the
215 ones with larger variance. This step was required to reduce the number of colors to a value that made
216 the computational load manageable by the hierarchical clustering. As a side effect, less relevant colors
217 (potential outliers) were cancelled by this approach. The selected (a^*, b^*) pairs were used to build a
218 dendrogram (based on the Euclidean distance). This structure expresses a hierarchical subdivision of
219 colors that can be cut at different levels to obtain different number of clusters (different color
220 quantizations). A first subdivision identified two (a^*, b^*) pairs that separated the white pixels (W)
221 from the red ones (R), producing an image segmentation such as the one shown in Fig. 6A-B.

222 Using a second subdivision, the W and R regions were further divided in two components. In detail W
223 and R were divided in a dark (W1 or R1) and a light (W2 or R2) component. In the Fig. 6C the second
224 segmentation on the W component is reported. Average values of L^*, a^*, b^* , on these regions and their
225 percentage with respect to the product's surface were considered as potential features to evaluate the
226 quality level of fresh-cut radicchio.

227

228 2.4. *Statistical analysis*

229 The effects of QL on the color features extracted by CVS on the fresh-cut radicchio samples were
230 evaluated performing a one-way ANOVA with data means arranged in a completely randomized
231 design. The mean values for QL were separated using the Student-Newman-Keuls (SNK) test. T-test
232 was performed by using Statistica 6.0 (StatSoft, 2001).

233

234 **3.0. RESULTS AND DISCUSSION**

235

236 *3.1. Advantages of proposed method in pre-processing phases and automatic color segmentation*

237

238 The procedures proposed in this paper brought advantages to several steps of the image processing
239 chain: color-chart detection and extraction, foreground separation and color-based product's
240 segmentation for product classification. When processing each image, in the first step the color-chart
241 was automatically detected, extracted and analyzed. The proposed method did not make any
242 assumption on position and orientation of the color-chart in the scene and can be applied in any
243 context in which it is useful to use a color reference in the image. The second step of image
244 processing was to separate the product (foreground) from the background, including in the foreground
245 as much product as possible and avoiding misclassification of background pixels as parts of the
246 foreground. In fact, the latter error could affect the statistical measures made on the product and
247 reduce the reliability of the CVS. All the methods that separates foreground and background rely on
248 some thresholds on features that can be related to every pixel individually (grey-level, color channels,
249 NIR data, etc) or that can be associated to properties of neighboring pixels (distance of grey-levels or
250 colors, gradients, texture properties, etc). Setting these thresholds often involves human intervention
251 and trial-and-error phases (Wu & Sun, 2013b). In this paper the threshold to separate the region of
252 interest was automatically determined using a fully data-driven approach. By applying, this approach,
253 some small areas of product were erroneously classified as background. However the experimental
254 results showed that missing these tiny regions did not affect quality and robustness of results. Instead,
255 the erroneous inclusion of background regions in the evaluation of statistical measures would have

256 produced larger effects on the stability of results. The proposed procedure was applied to the fresh-cut
257 radicchio, characterized by a nonuniform color, so the product surface needed to be segmented into its
258 most significant parts. Indeed, in the case of products with nonuniform color, the separation of the
259 whole surface into regions associated to relevant colors is very important (Balaban, 2008) but, at the
260 date, no well assessed and no robust solutions are available (Wu & Sun, 2013a). In this case, the
261 hierarchical clustering-based approach identified two macro areas: the mostly white one (W) and the
262 red one (R). The proposed approach did not required human intervention to initialize clusters or to set
263 the desired number of colors. The hierarchical structure was produced without such a-priori
264 information and the best cutting level of the dendrogram was decided on the base of the performance
265 reached by the produced color quantization in the classification and estimation phases.

266
267 *3.2. Color feature selection for quality level evaluation of fresh-cut radicchio during storage in air*
268 *and modified atmosphere by applying the proposed automatic procedure.*
269

270 In fresh-cut radicchio, the analysis of the NH_4^+ content allowed to improve the sensory evaluation of
271 QL, discriminating significantly three class of quality: high (ranging from QL=5 to QL=4), middle
272 (from QL =3 to QL =2) and poor (QL=1) (Table 1). As previously widely reported (Pace at al., 2014a;
273 Cefola et al., 2015) NH_4^+ is a chemical objective indicator of fruits and vegetable quality, useful to
274 standardize the sensory evaluation of visual quality performed through rating scale (Pace et al.,
275 2014b). The color features (L^* , a^* , b^*) obtained from the entire image of fresh-cut radicchio, using the
276 CVS significantly affected the QL. However, only two classes were identified by L^* parameters (QL=
277 5 and 4 from QL =3, 2, 1), while a^* allowed to discriminate only fresh samples (QL=5) from the
278 others quality levels. Finally, a no adequate discrimination was performed by b^* parameter (Table 1).
279 Thus, working on the entire images (without segmenting regions with different colors) produced an
280 insufficient or improper QL classification. This is due to the nonuniform color of fresh-cut radicchio,
281 that makes difficult the quantitative analysis of color (Wu & Sun, 2013a). The application of the fist

282 segmentation to the entire images of fresh-cut radicchio, allowed to obtain two color component,
283 named W or R. The color features (L^* , a^* , b^*) extracted from each component, affected significantly
284 the QL (Table 1).

285 Considering the W component, the L^* parameter allowed to differentiate two class of quality (QL= 5
286 and 4 from QL =3, 2, 1) as previously reported considering the color parameters extracted from the
287 non segmented images. The information provided by the lightness channel L^* , as verified in
288 previously works (Pace et al., 2011; 2013; 2014a), is less reliable: it strongly depends on the geometry
289 between observed surface, lights and sensor. The color parameter a^* allowed the best discrimination
290 of the QL in three quality class, matching the results obtained by NH_4^+ (Table 1). An inadequate
291 discrimination was performed by the b^* parameter (Table 1). The color parameters obtained from the
292 red component showed significant changes mainly associated to the variability among samples and
293 not related to visual quality loss. Indeed, during storage, the loss of visual quality of fresh-cut
294 radicchio is principally due to oxidative phenomena occurring on the white component as occur in
295 different fresh-cut vegetables (Wojciech et al., 2014).

296 The second segmentation, allowed to further split in two more color components both the W and R
297 parts of fresh-cut radicchio images. On the W part two components were automatically selected: a
298 dark white, W1, and a light white, W2. The L^* , a^* and b^* mean values of the colors associated to each
299 part were respectively: 56.97 (\pm 3.66), 2.60 (\pm 0.57) and 10.45 (\pm 0.45) in W1 and 60.23 (\pm 3.73),
300 2.04 (\pm 0.55) and 4.75 (\pm 0.62) in W2. The color parameters extracted from W1 and W2 resulted
301 significantly different for $P < 0.001$ ($n=120$), performing a *t*-test.

302 The percentages of W1 and W2 components were calculated with respect to the white part (W) and
303 with respect to the entire surface (I) of radicchio samples: if N^{W1} , N^{W2} , and N^W denote the number of
304 pixels corresponding to the W1, W2 and W regions, these percentage were N^{W1}/N^W and N^{W2}/N^W . In
305 the same way N^{W1}/N^I and N^{W2}/N^I represent the percentages of W1 and W2 with respect to the whole
306 surface of product (composed by N^I pixels). These percentages significantly affected the QL (Table

307 2). In detail, N^{W1}/N^W allowed to separate only samples with QL=5 from the other QL; while N^{W1}/N^I
308 was able to separate samples with QL=5 from radicchio pieces belonging to QL of 4, 3 and 2.
309 Unexpectedly, N^{W1}/N^I provided the same values for QL = 1 and QL=5 . This could be due to the
310 similarity between very dark red and the background: in fact the number of pixels dark white that
311 moves from QL=5 to QL=1 (due to browning) could be compensated by the pixels that become so
312 dark to be confused with the background.

313 N^{W2}/N^W allowed to discriminate only QL=5 samples from the other QL; whereas N^{W2}/N^I , provided a
314 good and significant discrimination of QL, matching the quality classes selected by NH_4^+ (Table 2).
315 Thus, the percentage of W2 (light white) tends to decrease from QL =5 to QL = 1, discriminating the
316 fresh-cut radicchio quality levels. Indeed, color is used as an indicator of quality for many fruits and
317 vegetable (Wu & Sun, 2013a) and bright and white color of fresh-cut radicchio samples is considered
318 as a freshness indicator by consumers. During storage, biochemical phenomena (such as enzymatic
319 and not enzymatic oxidation), also induced by cutting (Kader, 2002), cause color change which affect
320 the radicchio visual appearance: the main color changes regard the white part, which tends to become
321 darker. Similarly, in fresh-cut iceberg, the main color changes affecting consumer assessment of
322 visual quality were based on the white parts which turns to brown during storage (Pace et al., 2014a).

323 Considering separately the samples stored in AIR or pMA at the end of storage, the application of the
324 automatic procedure proposed showed that a^* of the W part (the complete white part of the product)
325 and the percentage N^{W2}/N^I , as the most discriminating color features of QL in fresh-cut radicchio
326 (Table 1 and 2). At the end of the storage, fresh-cut radicchio stored in AIR showed an a^* mean value
327 of 2.98 (\pm 0.36) significantly different ($p < 0.001$) from the mean value obtained on pMA samples
328 (2.1 \pm 0.38). These samples differed significantly also for the N^{W2}/N^I percentage which resulted 18.0
329 % (\pm 2.3) in pMA and 12.5% (\pm 3.2) in AIR samples. By comparing these values (a^* and N^{W2}/N^I
330 percentage) with that one reported in Tables 1 and 2, it can be noted that pMA samples at the end of
331 the storage reach a middle quality (from QL =3 to QL =2), while AIR samples reach the poor quality

332 class (QL =1). A good match with the scores attributed by sensory evaluation was showed: at the end
333 of storage samples stored in pMA or AIR were scored 3.0 (\pm 0.3) and 1.0 (\pm 0.18) respectively. In
334 fresh-cut radicchio stored in pMA bags (containing at the equilibrium 10% O₂ and 7% CO₂), the
335 browning of the white part was delayed. This accords with the general acknowledge that the use of
336 low levels of O₂ and high concentrations of CO₂, in combination with low storage temperatures,
337 represent the optimal conditions for storing fresh-cut vegetables, maintaining sensorial quality
338 (Jacxsens et al. 2000; Hempel, et al., 2013).

339

340 **4.0. Conclusion**

341

342 The paper addresses the development of CVS for the automatic color analysis of fruit and vegetables:
343 the goal of the system is to evaluate non-destructively the quality level of products. In particular the
344 proposed procedures involves new methodologies that reduce the human effort and subjectivity
345 required to design a CVS and to optimize its performance. The parameters controlling the image
346 processing algorithms are automatically set using data driven approaches instead of being fixed by
347 expert operators. A new technique is described that automatically locates the color-chart in the
348 images: a critical step to evaluate and reduce the error in color measuring due to unavoidable
349 instabilities of the CVS. A new approach is proposed to separate foreground and background: a region
350 growing method based on adaptive thresholds derived from the images is used to select most of the
351 product surface avoiding the inclusion of misclassified background pixels. Finally, relevant colors
352 best suited to effectively characterize a specific product are autonomously identified using a
353 hierarchical clustering approach that proved to be successful also on products characterized by
354 nonuniform colors. Hierarchical clustering is completely data-driven and do not suffer from
355 initialization problems or from the setting of the desired number of colors. It produces a structure
356 (dendrogram) that can be exploited by the CVS to check several color quantizations (associated with
357 different number and kind of colors). The system tests each possibility using its performance in

358 distinguishing the quality levels during the following classification and estimation steps. Each color
359 quantization is derived from the dendrogram by simply dynamically moving up or down on the
360 hierarchical structure. The resulting CVS proved to be effective in separating the quality classes of
361 interest on the fresh-cut radicchio.

362 The proposed approach allows the CVS to be easily applied to different products, with nonuniform
363 surface color (variable number and kind of colors. This significantly simplifies its practical
364 application in food processing with a reduced and less critical human intervention for its
365 configuration.

366

367 **Acknowledgments**

368 This research was financed by MIUR (Research Projects: ‘Smart Cities and Communities and Social
369 Innovation Prot. 84/Ric 02/03/2012, PON4a2_ Be&- Save). The authors thank Arturo Argentieri for
370 the technical support to the configuration of the experimental set-up.

371

372 **References**

- 373 Avila, F., Mora, M., Oyarce, M., Zuñiga, A., & Fredes, C. (2015). A method to construct fruit
374 maturity color scales based on support machines for regression: Application to olives and grape
375 seeds. *Journal of Food Engineering*, 162, 9-17.
- 376 Balaban, M. O. (2008). Quantifying nonhomogeneous colors in agricultural materials part I: method
377 development. *Journal of Food Science*, 73(9), 431-437.
- 378 Cefola, M., & Pace, B. (2015). Application of oxalic acid to preserve the overall quality of rocket and
379 baby spinach leaves during storage. *Journal of Food Processing and Preservation*.
380 doi:10.1111/jfpp.12502.
- 381 Hempel, A., O'Sullivan, M. G., Papkovsky, D. B., & Kerry, J. P. (2013). Nondestructive and
382 continuous monitoring of oxygen levels in modified atmosphere packaged ready-to-eat mixed salad
383 products using optical oxygen sensors, and its effects on sensory and microbiological counts during
384 storage. *Journal of Food Science*, 78(7), 1057-1062.
- 385 Hernández-Carrión, M., Hernando, I., Sotelo-Díaz, I., Quintanilla-Carvajal, M. X., & Quiles, A.
386 (2015). Use of image analysis to evaluate the effect of high hydrostatic pressure and pasteurization
387 as preservation treatments on the microstructure of red sweet pepper. *Innovative Food Science &*
388 *Emerging Technologies*, 27, 69-78.
- 389 Jacxsens, L., Devlieghere, F., De Rudder, T., & Debevere, J. (2000). Designing equilibrium modified
390 atmosphere packages for fresh-cut vegetables subjected to changes in temperature. *LWT – Food*
391 *Science and Technology*, 33, 178–87.
- 392 Kader, A. A. (2002). Biology and technology: An overview. *Postharvest Technol. Hortic. Crops*,
393 3311, 39-48.
- 394 Kang, S. P., East, A. R., & Trujillo, F. J. (2008). Colour vision system evaluation of bicolour fruit: A
395 case study with 'B74' mango. *Postharvest Biology and Technology*, 49(1), 77-85.

- 396 Kordecki, A., & Palus, H. (2014). Automatic detection of colour charts in images. *Przegląd*
397 *Elektrotechniczny*, 90(9), 197-202.
- 398 Manninen, H., Paakki, M., Hopia, A., & Franzén, R. (2015). Measuring the green color of vegetables
399 from digital images using image analysis. *LWT-Food Science and Technology*.
400 doi:10.1016/j.lwt.2015.04.005
- 401 Nunes, M. C. N., Emond, J. P., Rauth, M., Dea, S., & Chau, K. V. (2009). Environmental conditions
402 encountered during typical retail display affect fruit and vegetable quality and amount of waste.
403 *Postharvest Biology and Technology*, 51, 232–241.
- 404 Nunes, M. C. N. (2015). Correlations between subjective quality and physicochemical attributes of
405 fresh fruits and vegetables. *Postharvest Biology and Technology*, 107, 43-54.
- 406 Otsu, N. (1975). A threshold selection method from gray-level histograms. *Automatica*, 11, 23-27.
- 407 Pace, B., Cefola, M., Renna, F., & Attolico, G. (2011). Relationship between visual appearance and
408 browning as evaluated by image analysis and chemical traits in fresh-cut nectarines. *Postharvest*
409 *Biology and Technology*, 61(2), 178-183.
- 410 Pace, B., Cefola, M., Renna, F., Renna, M., Serio, F., & Attolico, G. (2013). Multiple regression
411 models and Computer Vision Systems to predict antioxidant activity and total phenols in
412 pigmented carrots. *Journal of Food Engineering*, 117(1), 74-81.
- 413 Pace, B., Cefola, M., Da Pelo, P., Renna, F., Attolico, G. (2014a). Non-destructive evaluation of
414 quality and ammonia content in whole and fresh-cut lettuce by computer vision system. *Food*
415 *Research International*, 64, 647-655.
- 416 Pace B., Cardinali A., D'Antuono I., Serio F., Cefola M. (2014b). Relationship between quality
417 parameters and the overall appearance in lettuce during storage. *International Journal of Food*
418 *Processing and Technology*, 1, 18-26.
- 419 StatSoft, I. N. C. (2001). STATISTICA (data analysis software system), version 6. Tulsa, USA, 150.
- 420

- 421 Wojciech, J., Florkowski, R. L., Shewfelt, B. B., & Stanley, E. P. (2014). *Postharvest handling. A*
422 *systems approach* (2nd ed., pp. 153–204). Amsterdam: Elsevier.
- 423 Wu, D., & Sun, D. W. (2013a). Colour measurements by computer vision for food quality control—A
424 review. *Trends in Food Science & Technology*, 29(1), 5-20.
- 425 Wu, D., & Sun, D. W. (2013b). Advanced applications of hyperspectral imaging technology for food
426 quality and safety analysis and assessment: a review – Part I: Fundamentals. *Innovative Food*
427 *Science and Emerging Technologies*, 19, 1-14.
- 428 Zhang, B., Huang, W., Li, J., Zhao, C., Fan, S., Wu, J., & Liu, C. (2014). Principles, developments
429 and applications of computer vision for external quality inspection of fruits and vegetables: A
430 review. *Food Research International*, 62, 326-343.
- 431 Zhang, B., Huang, W., Gong, L., Li, J., Zhao, C., Liu, C., & Huang, D. (2015). Computer vision
432 detection of defective apples using automatic lightness correction and weighted RVM
433 classifier. *Journal of Food Engineering*, 146, 143-151.
- 434

435 **Figure Captions**

436 **Figure 1.** The X-Rite color-chart used in the experiments. It provides a set of grey levels on the
437 bottom row. Several colors, properly distributed in the color space, allow the evaluation of color
438 fidelity of the acquisition system: the expected $L^* a^* b^*$ values are provided by the manufacturer.

439

440 **Figure 2.** A typical acquired image (A) before the processing to automatically detect the color-chart.
441 The two lightest greys are detected (B) and provide the required information about position and
442 attitude of the color-chart. Then all the other patches are identified and isolated (C). Now the color-
443 chart is removed (D) to simplify the following processing.

444

445 **Figure 3.** The purple lines represent a typical histogram of color distances measured over the whole
446 image between a pixel and its 8-neighborings. The significant peak (around zero) relates to distances
447 measured over mostly homogeneous regions: they are approximated by a normal distribution (fit_1 , red
448 line). A second peak (fit_2 , brown line) is related to the distances occurring at the edges between
449 foreground and background: this distribution allows the set of the threshold used by the growing
450 process to the value $\mu_2 - \sigma_2/2$. This choice does not include some pixels belonging to the product's
451 surface but prevents any background pixel from being erroneously classified as foreground.

452

453 **Figure 4.** The picture (A) shows typical starting regions used to separate foreground from
454 background: a very conservative threshold is used that does not need to be adapted to different
455 products or acquisition conditions. In fact, (B) shows that this conservative approach avoids any
456 misclassification of background pixels but selects a very limited part of the product's surface. In a
457 second phase of the processing, these starting regions grow to include neighboring pixels whose
458 distance is lower than the threshold automatically set using the histogram of distances. This produces

459 the final mask (C) that, as shown in (D), selects most of the product's surface: this pixels are used for
460 further processing.

461

462 **Figure 5.** The two-dimensional histogram of color (related to the a^* and b^* channels of the $L^*a^*b^*$
463 color space). The L^* is not considered because proved to be less stable and significant to characterize
464 colors. These representations, derived from each image, enable the identification of the most relevant
465 colors. The hierarchical clustering applied on these colors selects their quantization best suited to
466 separate the quality levels.

467

468 **Figure 6.** The surface of the fresh-cut radicchio shown in image (A) is separated into its white and red
469 regions (B) using the first level of the dendrogram structure produced by the hierarchical clustering.
470 The approach is completely data driven and does not require any setting based on heuristics or on a-
471 priori knowledge. The white region of radicchio is further segmented using the next level of the
472 dendrogram (C). The approach separates the light white and the dark white regions without any
473 further processing: all the possible color quantization are coded into the hierarchical structure and can
474 be dynamically explored to identify the most significant and best performing colors.

475

Figure 1

1	2	3	4	5	6
7	8	9	10	11	12
13	14	15	16	17	18
19	20	21	22	23	24

Figure 1.

Figure 2

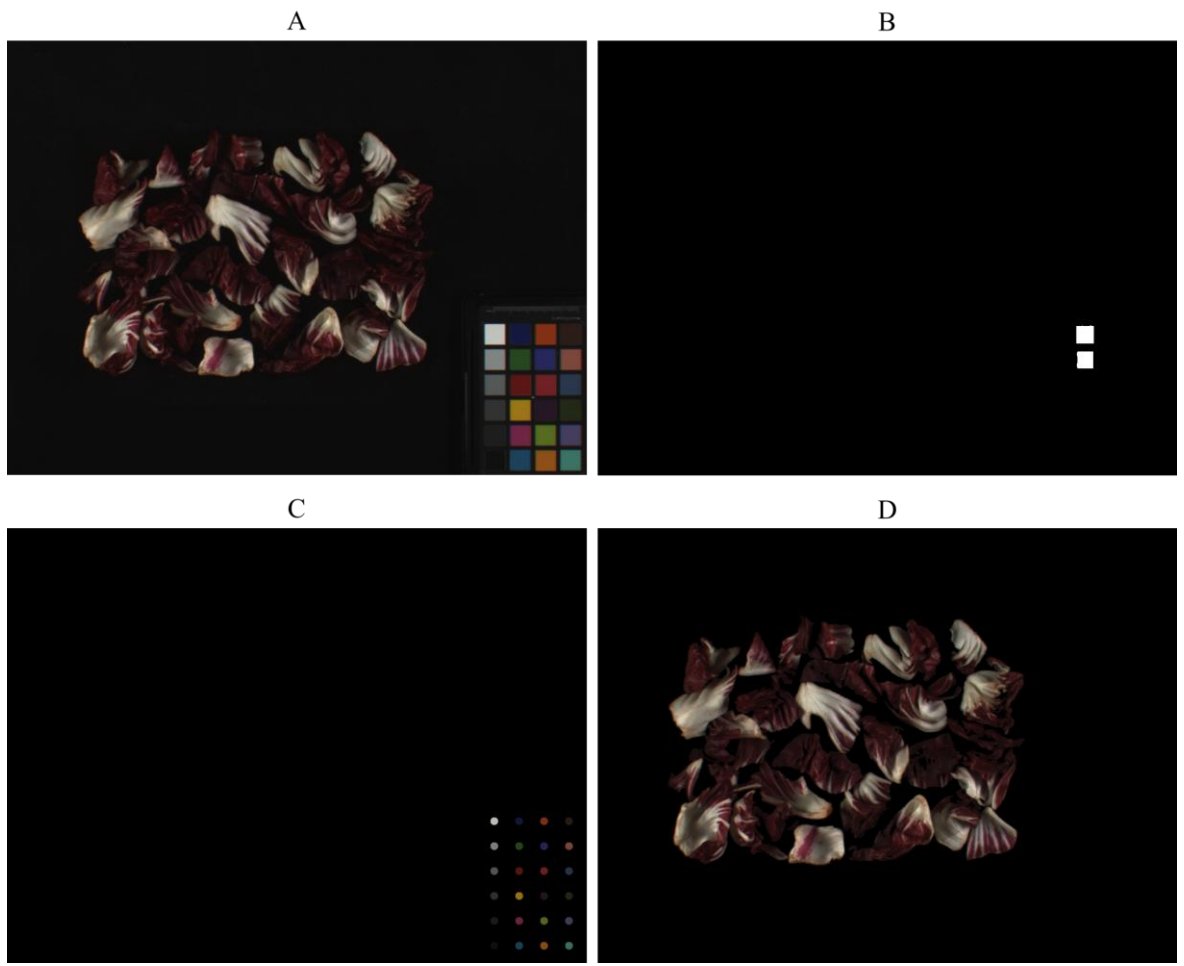


Figure 2.

Figure 3

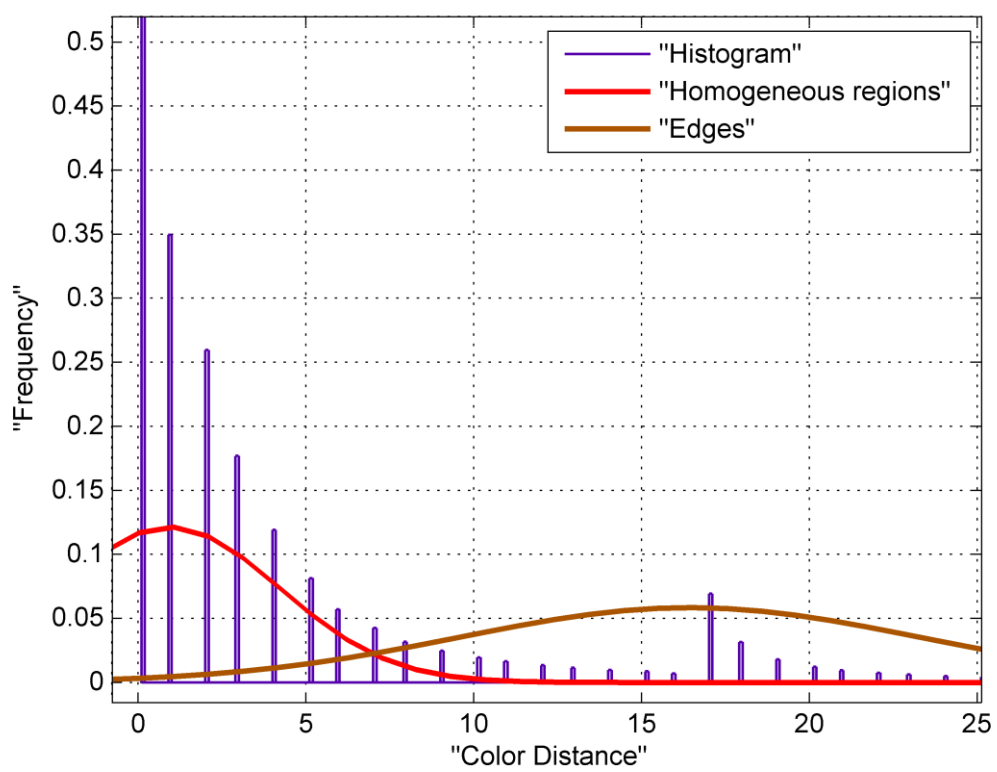


Figure 3.

Figure 4

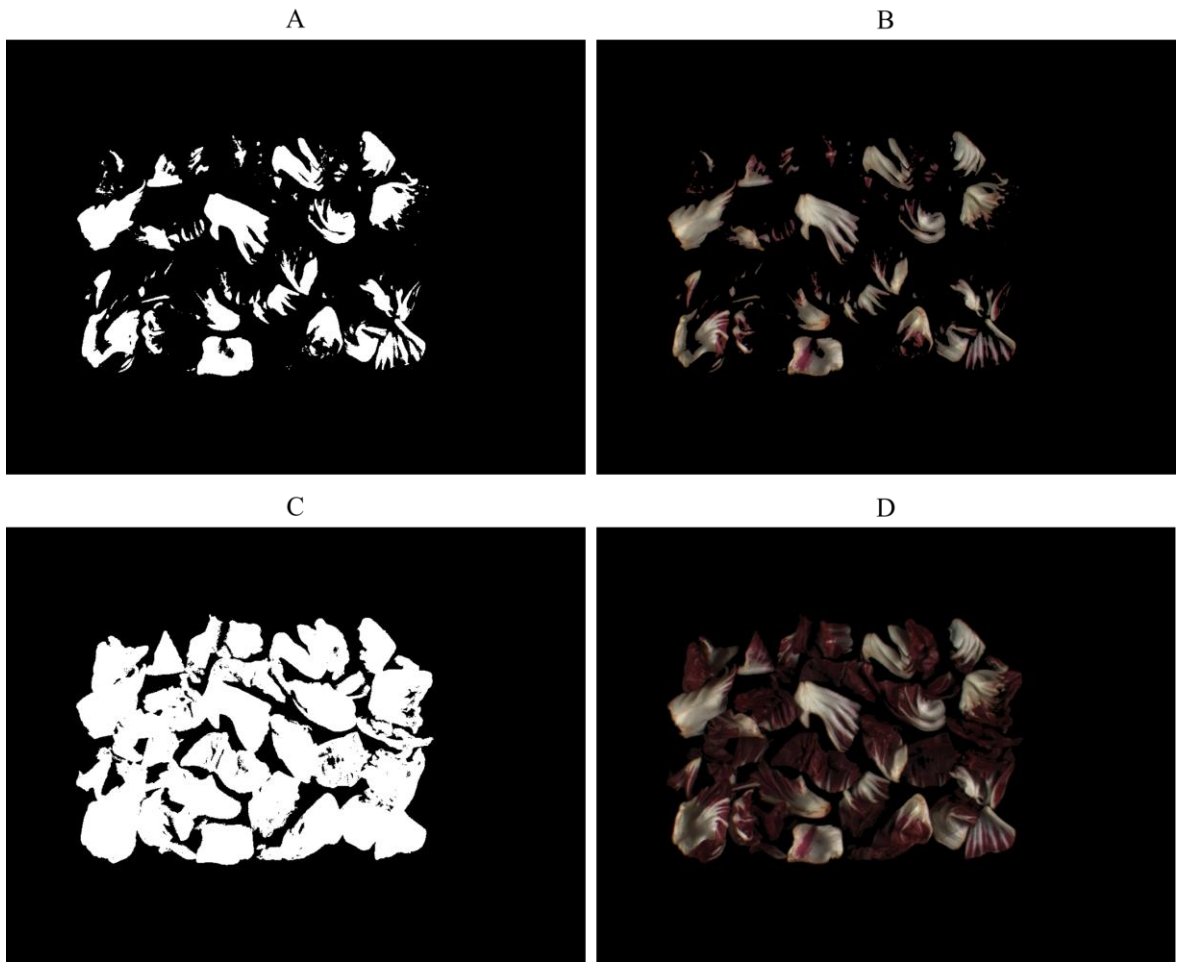


Figure 4.

Figure 5

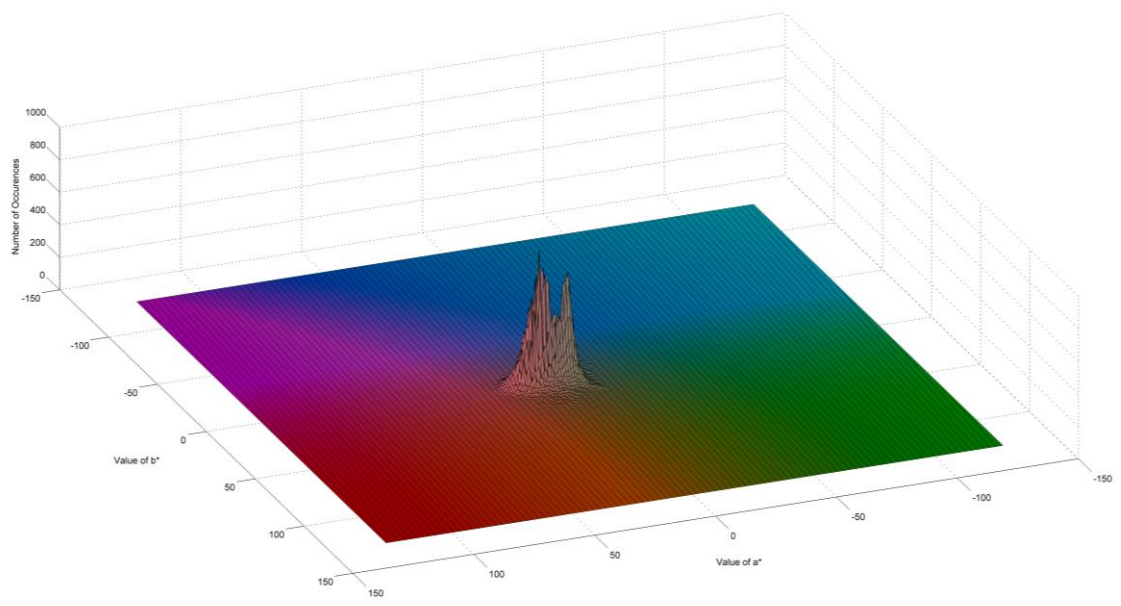


Figure 5.

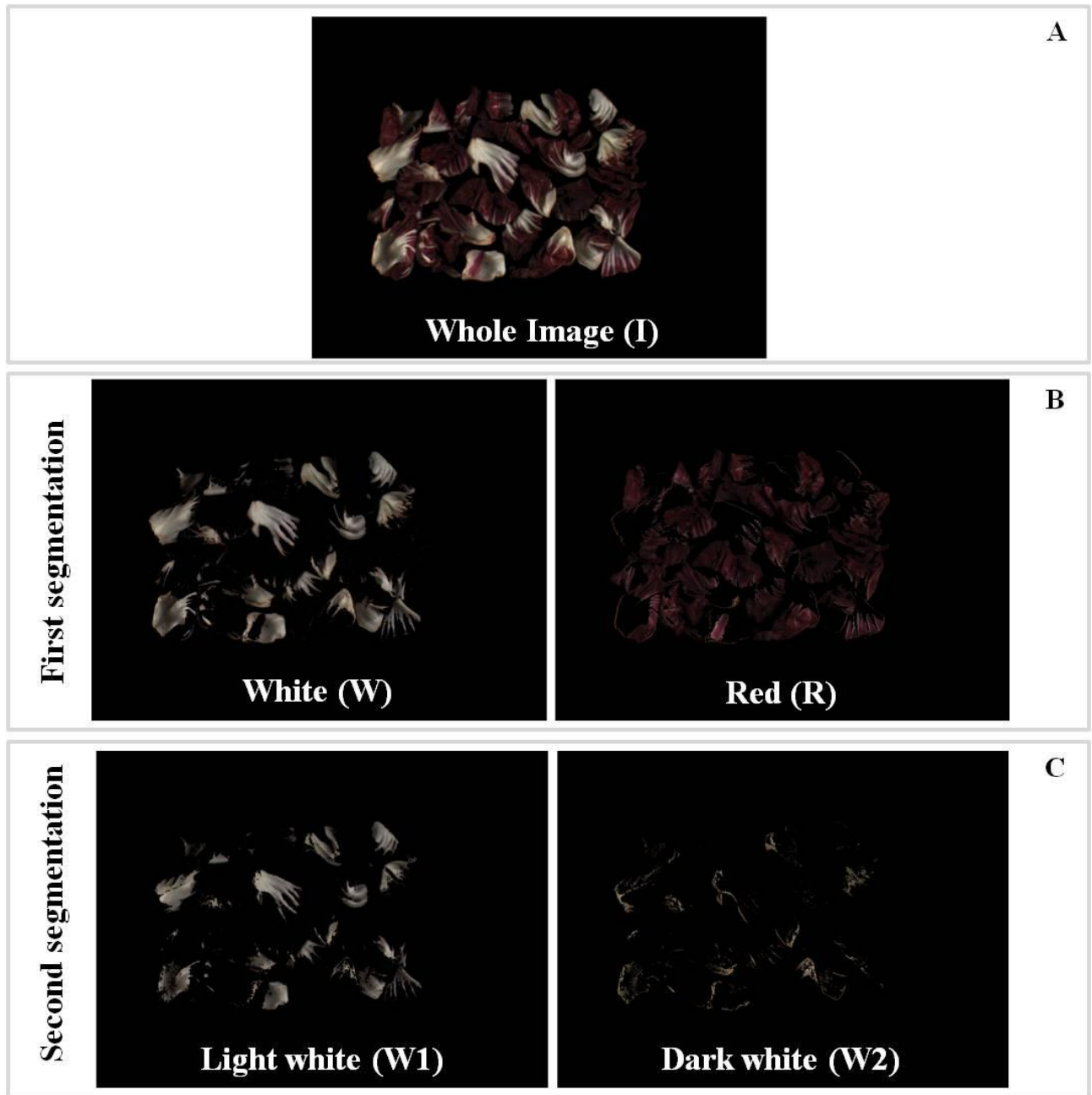


Figure 6.

Table 1. Main effects of quality levels (very good, good, acceptable, poor and very poor) on the ammonium (NH_4^+ $\mu\text{mole/g}$) and colour features (L^* , a^* and b^*) automatically extracted from the entire and segmented images by computer vision system in fresh-cut radicchio.

Fresh-Cut Radicchio Images		Very good	Good	Acceptable	Poor	Very poor	<i>P</i> value
		5	4	3	2	1	
	NH_4^+	0.07 c	0.10 c	0.22 b	0.30 b	0.66 a	***
Entire Image	L^*	41.63 a	40.59 a	37.10 b	37.50 b	35.75 b	***
	a^*	11.12 a	10.56 b	10.62 b	10.67 b	12.15 b	***
	b^*	4.41 c	4.97 b	5.58 a	5.54 a	5.10 b	***
<i>I segmentation</i>							
White (W)	L^*	64.07 a	61.96 a	53.56 b	59.15 b	58.65 b	***
	a^*	1.56 c	1.66 c	2.21 b	2.13 b	2.69 a	***
	b^*	4.90 c	5.59 b	6.47 a	6.37 a	6.08 ab	***
Red (R)	L^*	32.20 a	32.07 ab	30.89 c	31.03 bc	31.08 c	**
	a^*	16.98 a	16.16 b	14.85 c	15.17 c	15.91 b	***
	b^*	4.64 c	5.07 bc	5.54 a	5.48 a	5.02 b	***

Mean values of 6 replicates. For each parameter the mean values followed by different letters, are significantly different (P -value < 0.05) according to Student-Newman-Keuls (SNK) test.

Significance: **and *** = significant at P -value ≤ 0.01 and 0.001 , respectively.

Table 2. Main effects of quality levels (very good, good, acceptable, poor and very poor) on the percentages (%) of the W1 (dark component of the white part) and W2 (clear component of the white part) components calculated as number of pixel of each component on the white part W (N^{W1}/N^W or N^{W2}/N^W) or on the entire surface image (I) (N^{W1}/N^I or N^{W2}/N^I) of fresh-cut radicchio images.

White components percentages (%)	Very good 5	Good 4	Acceptable 3	Poor 2	Very poor 1	<i>P</i> value
N^{W1}/N^W	14.02 b	21.8 a	27.63 a	27.2 a	25.36 a	***
N^{W1}/N^I	4.44 b	7.24 a	6.99 a	7.34 a	4.50 b	***
N^{W2}/N^W	85.98 a	78.2 b	72.37 b	72.8 b	74.63 b	***
N^{W2}/N^I	28.88 a	26.3 a	19.09 b	19.6 b	13.33 c	***

Mean values of 6 replicates. For each parameter the mean values followed by different letters, are significantly different (P -value < 0.05) according to Student-Newman-Keuls (SNK) test.

Significance: *** = significant at P -value \leq 0.001.